

Unconventional Plasticity of HIV-1 Reverse Transcriptase: How Inhibitors Could Open a Connection “Gate” between Allosteric and Catalytic Sites

Luca Bellucci,^{†,‡} Lucilla Angeli,[†] Andrea Tafi,[†] Marco Radi,^{†,§} and Maurizio Botta^{†,||,*}

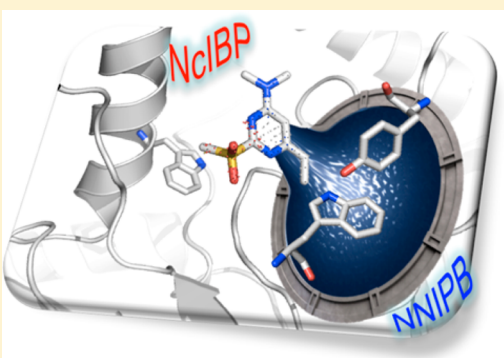
[†]Dipartimento di Biotecnologie, Chimica e Farmacia, Università degli Studi di Siena, Via Aldo Moro 2, 53100 Siena, Italy

[‡]Centro S3, Istituto Nanoscienze Consiglio Nazionale delle Ricerche, CNR-NANO, via G. Campi 213/A, 41125 Modena, Italy

[§]Dipartimento di Farmacia, Università degli Studi di Parma, Viale delle Scienze, 27/A, 43124 Parma, Italy

^{||}Sbarro Institute for Cancer Research and Molecular Medicine, Center for Biotechnology, College of Science and Technology, Temple University, BioLife Science Building, Suite 333, 1900 N. 12th Street, Philadelphia, Pennsylvania 19122, United States

Supporting Information



ABSTRACT: Targeted molecular dynamics (TMD) simulations allowed for identifying the chemical/structural features of the nucleotide-competitive HIV-1 inhibitor DAVP-1, which is responsible for the disruption of the T-shape motif between Try183 and Trp229 of the reverse transcriptase (RT). DAVP-1 promoted the opening of a connection “gate” between allosteric and catalytic sites of HIV-1 RT, thus explaining its peculiar mechanism of action and providing useful insights to develop novel nucleotide-competitive RT inhibitors.

the polymerase active site near the base of the thumb in the p66 palm subdomain.^{1,2} Still today, RT remains one of the most attractive targets for the development of new anti-HIV drugs, and recent literature reports several examples of promising NNRTIs inhibiting RT wild type and most of the more common drug-resistant mutants.^{3–8} As confirmed by X-ray of RT co-crystallized with different NNRTIs and by computational studies,^{9–13} NNIBP exists only when an inhibitor is bound to the enzyme and its shape is closely related to both chemical and three-dimensional features of the inhibitors. NNRTIs binding to the NNIBP promotes unconventional structural rearrangements near the polymerase active site, which compromises the catalytic activity and arrests the viral replication.^{14,15} In 2006, indolopyridones (INDOPYs)^{8,16} (Figure 1) were reported as a family of compounds inhibiting

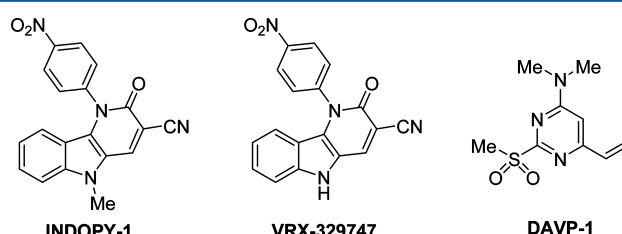


Figure 1. Chemical structure of known NcRTIs.

INTRODUCTION

The rapid replication of the HIV virus and its high error rate during this process cause resistant viruses to rapidly evolve in patients, making the development of a vaccine problematic and the discovery of new drugs particularly challenging. Consequently, there is an urgent need for new anti-HIV drugs acting with innovative mechanisms of action in order to fight viruses resistant to marketed antiviral drugs. Reverse transcriptase (RT) is an important target in antiretroviral therapy whose mechanism of action is still not completely understood.¹ Among the currently approved RT inhibitors, two different subclasses can be identified: the nucleos(t)ide RT inhibitors (NRTIs) and the non-nucleos(t)ide RT inhibitors (NNRTIs). NRTIs act at the catalytic site as chain terminators, whereas NNRTIs bind to an allosteric site, namely, the non-nucleoside inhibitors binding pocket (NNIBP), located at about 10 Å from

HIV-1 RT with a novel mechanism of action. A first striking feature of INDOPYs was their antiviral spectrum that was clearly distinct from that of NNRTIs and NRTIs. In addition, these compounds were competing with the nucleotide substrate but had no chain-termination mechanism, and the enzymatic inhibition was thus reversible and remained unaffected by most mutations altering the activity of NNRTIs and NRTIs.¹⁷ It was proposed to refer to this class of compounds as “nucleotide-competing RT inhibitors” (NcRTIs). Unfortunately, the precise location of the INDOPYs’ binding site was not identified so far, making it difficult for rational optimization of this promising class of inhibitors and clear comprehension of their mechanism of action. A few months after the first publication on the



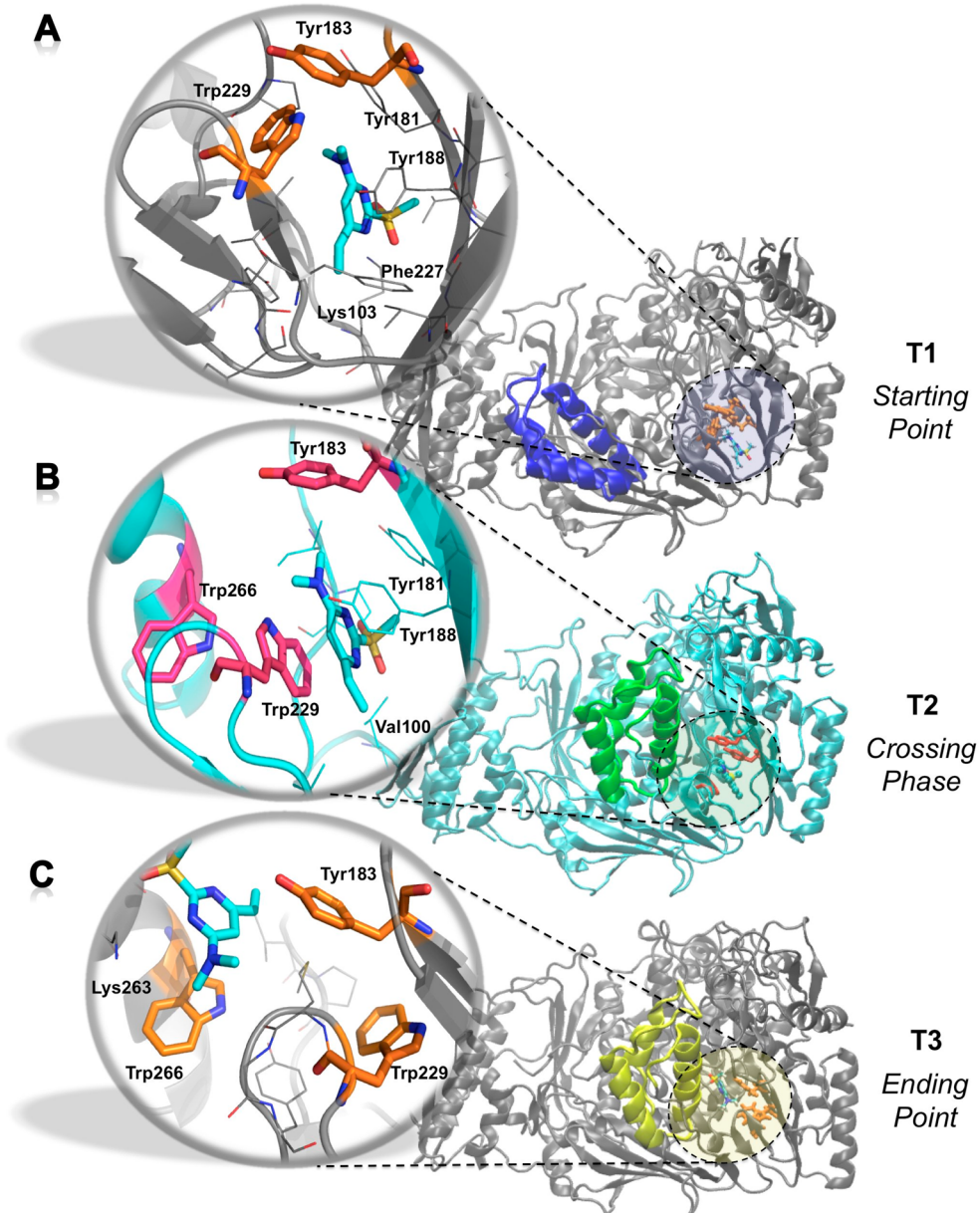


Figure 2. View of the starting, ending, and transition structures of the TMD simulation for the trajectory T1–T3. (A) Starting structure (T1): last frame of the 20 ns MD1 simulation of DAVP-1 docked within the NNIBP. (B) Representative snapshot of the crossing phase (T2) with DAVP-1 passing through the “gate”. (C) Ending structure (T3): last frame of the 20 ns MD2 simulation on the X-ray structure of DAVP-1 bound to the NcIBP (PDB code: 3ISN). For clarity, DAVP-1 and key residues Trp266, Tyr183, and Trp229 are shown as sticks, while the thumb subdomains are colored in blue, green, and yellow. The inset on the left shows a detailed view of the interactions between DAVP-1 and RT during the three key steps of the TMD simulation.

INDOPY derivatives, our research group reported the identification of an additional family of compounds classified as NcRTIs: the 4-dimethylamino-6-vinylpirimidines (DAVPs) (Figure 1).¹⁸ Despite the fact that DAVPs are structurally related to common NNRTIs (e.g., TNK-651),¹⁹ they showed a biological mechanism of action similar to that of INDOPYs even if with a different resistance profile.¹⁷ In addition, the peculiar kinetic of binding of DAVPs to RT, compared to the INDOPY derivatives, allowed us to solve the first crystallographic structure of a NcRTI (namely, DAVP-1) bound to the apo-RT (PDB: 3ITH and 3ISN); the NcRTIs binding pocket (NcIBP) was located within the hinge region, at the interface between the p66 thumb and palm subdomains in front of β 12– β 13 hairpin and close to the catalytic site.⁴ Nevertheless,

on the basis of the identified NcIBP, it was not possible to explain why DAVP-1 had a loss of activity toward the K103N and Y181I RT mutations,^{14,18,20} which are located within the NNIBP and usually negatively affect NNRTIs’ activity. It was interesting to note that a few crystallographic structures of RT/NNRTIs complexes (PDB: 1TV6, 2ZD1, 1KLM, and 2BSJ) showed a small hole between the polymerase site and the NNIBP.^{7,21–23} This peculiar structural feature has been also found in the structure of the TSAO-T/RT complex (PDB: 3QO9), and the authors suggested its possible exploitation for the design of NNRTIs able to reach the polymerase site^{24a} as it has been recently accomplished by Jorgensen and Anderson.^{24b}

On the basis of these findings and with the aim to rationalize the resistance profile of DAVP-1, we speculated⁴ that this

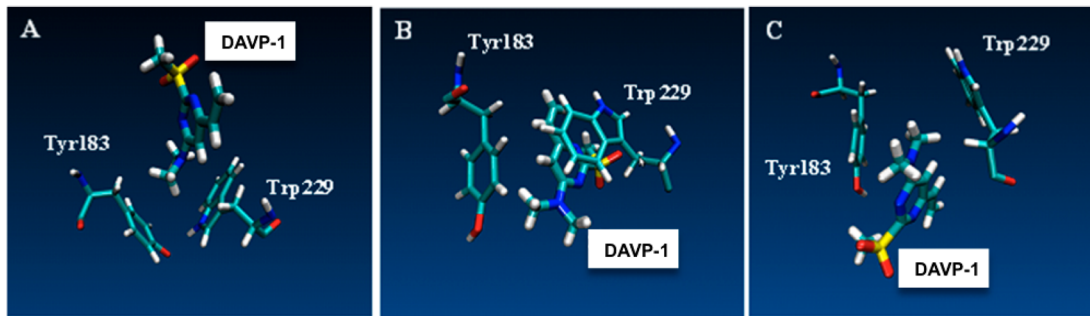


Figure 3. Spatial relationships between DAVP-1 and the “gate” during the crossing phase. (A) DAVP-1 is “knocking” at the “gate”: at the beginning of the TMD simulation, DAVP-1 starts to interact with the residues lining the gate (Tyr183 and Trp229). (B) DAVP-1 is opening the “gate”: after the insertion of the dimethylamino group between the side chains of Tyr183 and Trp229, DAVP-1 pushes these residues away from their original position and start to open the gate. (C) DAVP-1 has just crossed the “gate”.

compound “[...] could travel between the non-nucleoside- and nucleoside-binding pockets [...]” to exert its activity.

Herein, we have analyzed a putative mechanism of action according to which DAVP-1 would bind into the NNIBP and promote the opening of a “gate” between the NNIBP and the catalytic site to reach the NcIBP. Investigating such a mechanism by molecular dynamics simulations, we were able to describe how to promote the formation of a “channel” between the conventional NNIBP and the polymerase site as observed in other crystallographic structures cited above.^{7,21–24}

RESULTS AND DISCUSSION

We used the targeted molecular dynamics (TMD) technique, which is routinely used to study dynamical properties of proteins,¹⁹ to induce conformational changes from the structure of the RT with DAVP-1 docked into the NNIBP to the structure of the RT with DAVP-1 docked into NcIBP. During the TMD simulation, the ligand was forced to cross the portion of protein between the two sites, probing the plastic features of the NNIBP and highlighting the molecular mechanism that could promote a structural deformation between the allosteric and catalytic sites of HIV-1 RT.

To reach this goal, two preliminary MD simulations of 20 ns each were performed in explicit solvent: the first on the RT/DAVP-1 system with the inhibitor docked in the NNIBP¹⁸ (MD1) and the second on the inhibitor located in the NcIBP⁴ (MD2). The relaxed structures obtained from these preliminary simulations were then used to carry out the TMD simulation. The last conformation of the MD1 simulation, where DAVP-1 was bound into the NNIBP, was used as the initial point to perform the TMD (hereafter called “starting structure” or T1), while the last frame of the MD2 was chosen as the target structure (hereafter called “ending structure” or T3) (Figure 2A,C). A detailed description of the preliminary molecular dynamics simulations (MD1 and MD2) to obtain T1 and T3 is reported in the Supporting Information.

The conformations of the RT/DAVP-1 complexes T1 and T3 differ mainly in the location of DAVP-1 and in the conformation of the thumb subdomain. In particular, the thumb subdomain is in an open state in T1 and in a closed state in T3 (Figure 2A,C). Because DAVP-1 was supposed to move from T1 to T3, the TMD involved only the heavy atoms of DAVP-1 and the backbone’s atoms of the thumb: DAVP-1 was thus forced to travel from the NNIBP to the NcIBP, while the thumb domain was forced to change from the open to the closed state. TMD simulation was carried out for 20 ns using an

elastic constant of 35 kcal/(mol Å²) (for more details, see the Experimental Section), and we collected the main protein conformational changes that occurred between the NNIBP and the NcIBP zone. Analyses of the TMD simulation trajectory and protein–inhibitor interactions suggested dividing the crossing process of DAVP-1 in three phases, based on the position of the inhibitor with respect to the path between the two binding sites.

In the early stage of the TMD simulation (Phase I), DAVP-1 was confined into the NNIBP, and all the structural elements forming the pocket did not undergo essential changes. However, we observed that the thumb subdomain changed its conformation from an open to a closed state and remained closed until the end of the simulation (from T1 to T2, Figure 2A,B). Because of the high mobility of the thumb motif, the closure movement of the thumb that occurred at the early stage of the TMD was not surprising. In this phase, owing to the hydrophobic nature of both the NNIBP and the inhibitor, the interactions between DAVP-1 and RT were dominated by hydrophobic interactions (Figure 2A). The dimethylamino moiety of DAVP-1 gave profitable van der Waals contacts with side chains of Ile194, Tyr188, Tyr183, Trp229, Tyr181, and Pro95. The vinyl group was located in a lipophilic pocket lined by Leu234, Val106, and Phe227, where it established favorable nonpolar interactions, while the methyl bound to the sulfone group interacted with Val179 and Tyr181. Oxygen atoms of the sulfone group pointed toward the solvent making profitable interactions with water or, eventually, with Lys103. In particular, Lys103 is located at the solvent exposed portion of the proposed entry site of the NNIBP. As we and other authors suggested elsewhere, the K103N mutation negatively affects the activity of RT inhibitors (and also of DAVP-1) opposing resistance to the opening of the allosteric pocket (NNIBP) by the incoming inhibitor.^{9–11}

The pyrimidine ring of DAVP-1 was involved in a face-to-face π stacking interaction with the ring of Tyr188. During phase I, residues Trp229 and Tyr183 interacted each other in T-shape manner in which the NH of the indole ring of Trp229 points toward the aromatic ring of Tyr183. These two residues in the T-shape conformation mainly define the closed form of the “gate” between the two binding sites.

In phase II, we observed that the applied forces induced the DAVP-1 to open a “gate” between the catalytic site and NNIBP (T2, Figure 2B). Focusing our attention on the interactions between DAVP-1 and the “gate” residues (Tyr183 and Trp229) along this phase, it was possible to grasp the main interactions that drove the induced conformational changes during the

crossing phase (details in Figure 3). In phase II, DAVP-1 is forced to move toward the NcIBP, starting to insert the dimethylamino group, used as a sort of picklock, between the side chains of Trp229 and Tyr183. During this phase, the interaction between Trp229 and Tyr183 is compromised; the dimethylamino moiety pushes away Tyr183, whereas the DAVP-1 starts to interact with Trp229 (Figure 3A). In particular, the polar C5 hydrogen of the pyrimidine ring starts to point toward the ring of Trp229 originating an edge-to-face π stacking interaction.²⁵ It is worth noting that previously reported C5-substituted derivatives of DAVP-1 completely lost their antiviral activity thus underlining the importance of this edge-to-face π stacking interaction that could not be explained by simple SAR on the single putative binding sites (NNIBP and NcIBP).¹⁴ The synergism between the push action of the dimethylamino moiety and the favorable stacking interaction is therefore the driving force that promotes the disruption of the conserved T-shape motif between Trp229 and Tyr183 (Figure 3B,C) and is theoretically responsible for the antiviral activity of this class of compounds. In addition, Tyr188 and Tyr181 form a sort of platform that assists DAVP-1 during the approach and opening of the gate (Figure 4). It is worth noting that mutations of Tyr181 to bulky residues (i.e., Y181I) disrupt this platform negatively affecting the passage of DAVP-1.

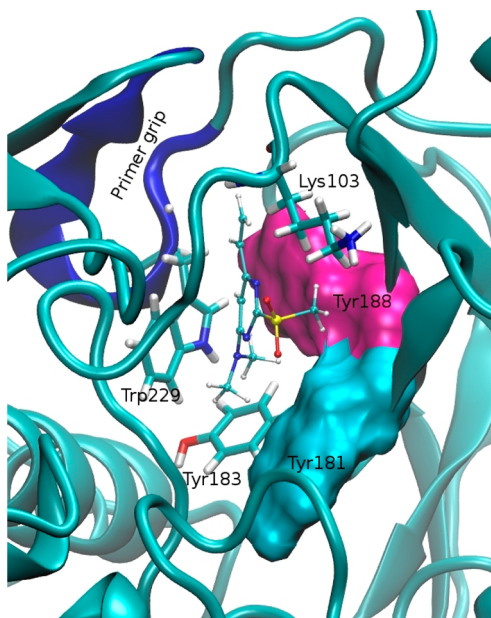


Figure 4. Snapshot from the TMD simulation at the beginning of phase II. Lys103 is not directly involved in the binding of the substrate and points toward the solvent. Tyr181 and Tyr188 form a flat platform which assists the approach of DAVP-1 to the “gate” residues (Trp229 and Tyr183).

In phase III, DAVP-1 has opened the “gate” and gradually moves toward the ending point (NcIBP) (Figure 2C). At the beginning of this phase (Figure 3C), the ligand is parallel to the aromatic rings of Tyr183 and Trp229, thus promoting favorable aromatic interactions. On the basis of the results of the present study, we do not exclude that the opening of the “gate” could represent the key step of the mechanism of action of DAVP-1, corroborating the hypothesis that it could travel between NNIBP and NcIBP as proposed in our previous work.⁴ This mechanism could justify the DAVP-1 loss of activity against the

two NNRTIs-related mutants K103N and Y181I, which are located at the entrance of the NNIBP and close to the connection “gate”, respectively, and that could thus prevent DAVP-1 from reaching the NcIBP. In addition, it is interesting to note that the proposed mechanism is based on disrupting the interaction of the two conserved residues Tyr183 and Trp229 (the “gate”). Because these residues are not prone to mutation by the HIV-1 virus, the proposed mechanism could be efficiently exploited to develop new DAVP-1 analogues able to overcome mutations that may compromise the binding to the NNIBP.

CONCLUSIONS

In summary, DAVP-1 was recently identified by our research group as belonging to the new class of NcRTIs.^{14,18} Because of its structural similarity with the NNRTI TNK-651¹¹ and for the loss of activity observed against the two most frequent mutations associated with NNRTIs resistance (K103N and Y181I), it was initially expected that these compounds would also behave as NNRTIs. However, DAVPs were found to inhibit HIV-1 RT by a competitive mechanism with the nucleotide substrate. In this context, the crystal complex of compound DAVP-1 and RT was solved at 2.5 Å resolution revealing a novel binding site, distinct from the NNIBP and close to the RT polymerase catalytic site. The presence of a series of crystallographic complexes in which there is evidently a channel between the NNIBP and the catalytic site (RT is a very flexible protein) persuaded us to study how the allosteric segment between the NNIBP and NcIBP could be “reshaped” when DAVP-1 is forced to travel across this region. By forcing the passage of DAVP-1 from the NNIBP to the NcIBP, the TMD gave an atomistic description on how to induce further conformational changes in the allosteric zone of the RT. In particular, we observed that the formation of the channel connecting the two binding sites is mainly regulated by the presence of a “gate” formed by Try183 and Trp229 in a T-shape conformation. The simulations highlighted that the push action of the dimethylamino moiety and favorable stacking interactions with Trp229 were the features of DAVP-1 responsible for the disruption of the T-shape motif and the consequent formation of the channel between the non-nucleoside- and nucleoside-binding pockets.

In conclusion, the induced travel of the DAVP-1 across the two binding sites highlighted that the NNIBP could be modeled far beyond the limits described for common NNRTIs. In particular, we identified the chemical/structural features of DAVP-1 responsible for the disruption of the T-shape motif between Try183 and Trp229 (opening of the connection “gate”), providing an innovative mechanism of action that should be exploited in developing novel small molecule inhibitors belonging to the NcRTIs family.

EXPERIMENTAL SECTION

Methods and Computational Details. System setup and classical MD were performed with NAMD (v2.7)²⁶ and VMD (v1.8.7)²⁷ software packages. The standard AMBER forcefield²⁸ was used for the protein, ligands, and counterions, and the TIP3P force field was used for water.²⁹ Atom types as well as bonded and nonbonded parameters were assigned to atoms by analogy or through interpolation from those already present in AMBER force field. To calculate partial atomic charges, DAVP-1 was optimized using the ab initio quantum chemistry

program GAMESS³⁰ at the B3LYP/6-311++G** level of theory. Consequently, a set of atom-centered HF/6-31G* charges was obtained for the inhibitor by application of RESP methodology.³¹ The system composed by RT and DAVP-1 was surrounded by a periodic box of water molecules, which were extended for at least 12 Å from the protein atoms. A total of five Cl ions were added to guarantee neutrality. The total number of water molecules in each system was 34,956 in a rectangular box of dimensions 126 Å × 88 Å × 117 Å. The rRESPA multiple time-step method³² was employed with 1.0 fs for bonded, 2.0 fs for the short-range part of the nonbonded, and 4.0 fs for the long-range part of the electrostatic forces.²⁵ The simulations were conducted using periodic boundary conditions (PBC), and the long-range part of the electrostatic was treated with the particle-mesh-ewald (PME) method,³³ with a grid size of 125 Å × 90 Å × 120 Å. The distance cut off for nonbonded interactions was set to 10 Å, and the switch function was applied to smooth interactions between 8 and 10 Å. All simulations were conducted in the NPT ensemble. The temperature was set to 310 K, and the Langevin thermostat was employed for temperature regulation.³⁴ The pressure was set to 1 atm and regulated via isotropic Langevin piston manostat.³⁵ The systems were submitted to 5000 steps of conjugate gradient geometry optimization with harmonic restraints on the protein heavy atoms using a force constant of 10 kcal/(mol Å²). After energy minimization, the system was submitted to 500 ps of MD simulation. The first 250 ps of MD were performed by applying harmonic restraints on the protein heavy atoms using a force constant of 10 kcal/(mol Å²). In the last 250 ps of MD, the force constant was scaled to 5 kcal/(mol Å²). Subsequently, 10,000 steps of minimization without restraints were performed. The final structures were then used as starting point for unrestrained molecular dynamics. MD simulations were carried out for 20 ns.

The final conformations were used to set up the targeted molecular dynamic. TMD was performed using as the starting point the last conformation obtained from the MD simulation of the system with DAVP-1 docked into the NNIBP (starting structure). The TMD target structure was the final conformation of the MD simulation of DAVP-1 bounded into its natural binding pocket (ending structure). The target atoms were the heavy atoms of the ligand and the backbone carbon atoms (C_α, C) of the RT thumb segment (residues 250 to 310 of the p66 subunit). The conformational changes occurred only in the part of p66 subunit involved in the formation of NNIBP. The p51 subunit and residues from 320 to the C-terminal of the p66 subunit did not undergo to conformational changes. This segment of the system, therefore, was restrained to the initial positions and used to align the initial structure to the target structure of the TMD simulation. The alignment was performed using the backbone heavy atoms. The obtained atoms coordinates were used as starting point for TMD simulation. The backbone heavy atoms used to align the initial structure to the target structure were restrained to the initial positions using harmonic restraints with a force constant of 0.1 kcal/(mol Å²). Restraints were maintained throughout the whole simulation to prevent translation and rotation of the system. The residues of the system between the NNIBP and the RT catalytic site (residues from 1 to 250 and residues from 310 to 320 of p66 subunit) were kept free to move. The heavy atoms of DAVP-1 and the backbone carbon atoms of the thumb subdomain were forced to move from the starting structure (DAVP-1 bound to NNIBP) to the ending structure

(DAVP-1 bound to the natural RT catalytic site). At each TMD step, the current target conformation was used to calculate the RMSD with respect to the final target conformation, defining the current RMSD(t) value. The force on each target atoms was obtained from the gradient of the harmonic potential as described in the TMD section of the NAMD manual. The elastic constant for TMD forces was set to 30 kcal/mol. The harmonic potential was calculated using the difference between the current RMSD(t) and a reference RMSD(0) value. The reference RMSD(0) values monotonically decreased from an initial value of 20 Å to a final value of 1.3 Å. Because part of the protein was restrained to the initial position, it was not necessary to align the structure with respect to the target structure at each step of TMD simulation. TMD simulation was carried out for 20 ns.

■ ASSOCIATED CONTENT

S Supporting Information

Details on MD1 and MD2 simulations to define the TMD starting point T1 and ending point T3, respectively. A movie made from the trajectory of the TMD simulation showing the initial phase of the “gate” opening. This material is available free of charge via the Internet at <http://pubs.acs.org>.

■ AUTHOR INFORMATION

Corresponding Author

*E-mail: botta.maurizio@gmail.com. Phone: +39 0577 234306. Fax: +39 0577 234306.

Notes

The authors declare no competing financial interest.

■ ACKNOWLEDGMENTS

This work was supported by the European Union: “CHAARM”, Collaborative Project, Grant HEALTHF3-2009-242135. We are grateful to Lead Discovery Siena Srl.

■ REFERENCES

- (1) Mehellou, Y.; De Clercq, E. Twenty-six years of anti-HIV drug discovery: Where do we stand and where do we go? *J. Med. Chem.* **2010**, *53*, 521–538.
- (2) Li, D.; Zhan, P.; De Clercq, E.; Liu, X. Strategies for the design of HIV-1 non-nucleoside reverse transcriptase inhibitors: Lessons from the development of seven representative paradigms. *J. Med. Chem.* **2012**, *55*, 3595–3613.
- (3) Jabbour, E.; Kantarjian, H. Chronic myeloid leukemia: 2012 update on diagnosis, monitoring, and management. *Am. J. Hematol.* **2012**, *87*, 1037–1045.
- (4) Freisz, S.; Bec, G.; Radi, M.; Wolff, P.; Crespan, E.; Angel, L.; Dumas, P.; Maga, G.; Botta, M.; Ennifar, E. Crystal structure of HIV-1 reverse transcriptase bound to a non-nucleoside inhibitor with a novel mechanism of action. *Angew. Chem., Int. Ed.* **2010**, *49*, 1805–1808.
- (5) Himmel, D. M.; Sarafianos, S. G.; Dharmasena, S.; Hossain, M. M.; McCoy-Simandle, K.; Ilina, T.; Clark, A. D., Jr.; Knight, J. L.; Julias, J. G.; Clark, P. K.; Krogh-Jespersen, K.; Levy, R. M.; Hughes, S. H.; Parniak, M. A.; Arnold, E. HIV-1 reverse transcriptase structure with RNase H inhibitor dihydroxy benzoyl naphthyl hydrazone bound at a novel site. *Chem. Biol.* **2006**, *1*, 702–712.
- (6) Jochmans, D.; Deval, J.; Kesteleyn, B.; Van Marck, H.; Bettens, E.; De Baere, I.; Dehertogh, P.; Ivens, T.; Van Ginderen, M.; Van Schoubroeck, B.; Ehteshami, M.; Wigerinck, P.; Götte, M.; Hertogs, K. Indolopyridones inhibit human immunodeficiency virus reverse transcriptase with a novel mechanism of action. *J. Virol.* **2006**, *80*, 12283–12292.
- (7) Pata, J. D.; Stirtan, W. G.; Goldstein, S. W.; Steitz, T. A. Structure of HIV-1 reverse transcriptase bound to an inhibitor active against

- mutant reverse transcriptases resistant to other nonnucleoside inhibitors. *Proc. Natl. Acad. Sci. U.S.A.* **2004**, *101*, 10548–53.
- (8) Zhang, Z.; Walker, M.; Xu, W.; Shim, J. H.; Girardet, J. L.; Hamatake, R. K.; Hong, Z. Novel nonnucleoside inhibitors that select nucleoside inhibitor resistance mutations in human immunodeficiency virus type 1 reverse transcriptase. *Antimicrob. Agents Chemother.* **2006**, *50*, 2772–2781.
- (9) Mugnaini, C.; Alongi, M.; Togninelli, A.; Gevariya, H.; Brizzi, A.; Manetti, F.; Bernardini, C.; Angelini, L.; Tafì, A.; Bellucci, L.; Corelli, F.; Massa, S.; Maga, G.; Samuele, A.; Facchini, M.; Clotet-Codina, I.; Armand-Ugón, M.; Esté, J. A.; Botta, M. Dihydro-alkylthio-benzyl-oxopyrimidines as inhibitors of reverse transcriptase: synthesis and rationalization of the biological data on both wild-type enzyme and relevant clinical mutants. *J. Med. Chem.* **2007**, *50*, 6580–6595.
- (10) Radi, M.; Maga, G.; Alongi, M.; Angelini, L.; Samuele, A.; Zanolini, S.; Bellucci, L.; Tafì, A.; Casaluce, G.; Giorgi, G.; Armand-Ugón, M.; Gonzalez, E. M.; Esté, J. A.; Baltzinger, M.; Bec, G.; Dumas, P.; Ennifar, E.; Botta, M. Discovery of chiral cyclopropyl dihydro-alkylthio-benzyl-oxopyrimidine (S-DABO) derivatives as potent HIV-1 reverse transcriptase inhibitors with high activity against clinically relevant mutants. *J. Med. Chem.* **2009**, *52*, 840–851.
- (11) Rodríguez-Barrios, F.; Balzarini, J.; Gago, F. The molecular basis of resilience to the effect of the Lys103Asn mutation in non-nucleoside HIV-1 reverse transcriptase inhibitors studied by targeted molecular dynamics simulations. *J. Am. Chem. Soc.* **2005**, *127*, 7570–7578.
- (12) Shen, L.; Shen, J.; Luo, X.; Cheng, F.; Xu, Y.; Chen, K.; Arnold, E.; Ding, J.; Jiang, H. Steered molecular dynamics simulation on the binding of NNRTI to HIV-1 RT. *Biophys. J.* **2003**, *84*, 3547–3563.
- (13) Zhou, Z.; Madrid, M.; Evanseck, J. D.; Madura, J. D. Effect of a bound non-nucleoside RT inhibitor on the dynamics of wild-type and mutant HIV-1 reverse transcriptase. *J. Am. Chem. Soc.* **2005**, *127*, 17253–17260.
- (14) Radi, M.; Falciani, C.; Contemori, L.; Petricci, E.; Maga, G.; Samuele, A.; Zanolini, S.; Terrazas, M.; Castria, M.; Esté, J. A.; Togninelli, A.; Clotet-Codina, I.; Armand-Ugón, M.; Botta, M. A multidisciplinary approach for the identification of novel HIV-1 non-nucleoside reverse transcriptase inhibitors: S-DABOCs and DAVPs. *ChemMedChem* **2008**, *3*, 573–593.
- (15) Zhan, P.; Liu, X.; Li, Z.; Pannecouque, C.; De Clercq, E. Design strategies of novel NNRTIs to overcome drug resistance. *Curr. Med. Chem.* **2009**, *16*, 3903–3917.
- (16) Das, K.; Bauman, J. D.; Clark, A. D., Jr.; Frenkel, Y. V.; Lewi, P. J.; Shatkin, A. J.; Hughes, S. H.; Arnold, E. High-resolution structures of HIV-1 reverse transcriptase/TMC278 complexes: Strategic flexibility explains potency against resistance mutations. *Proc. Natl. Acad. Sci. U.S.A.* **2008**, *105*, 1466–1471.
- (17) Maga, G.; Radi, M.; Gerard, M. A.; Botta, M.; Ennifar, E. HIV-1 RT inhibitors with a novel mechanism of action: NNRTIs that compete with the nucleotide substrate. *Viruses* **2010**, *2*, 880–99.
- (18) Maga, G.; Radi, M.; Zanolini, S.; Manetti, F.; Cancio, R.; Hübscher, U.; Spadari, S.; Falciani, C.; Terrazas, M.; Vilarrasa, J.; Botta, M. Discovery of non-nucleoside inhibitors of HIV-1 reverse transcriptase competing with the nucleotide substrate. *Angew. Chem., Int. Ed.* **2007**, *46*, 1810–3.
- (19) Hopkins, A. L.; Ren, J.; Esnouf, R. M.; Willcox, B. E.; Jones, E. Y.; Ross, C.; Miyasaka, T.; Walker, R. T.; Tanaka, H.; Stammers, D. K.; Stuart, D. I. Complexes of HIV-1 reverse transcriptase with inhibitors of the HEPT series reveal conformational changes relevant to the design of potent non-nucleoside inhibitors. *J. Med. Chem.* **1996**, *39*, 1589–1600.
- (20) Radi, M.; Petricci, E.; Maga, G.; Corelli, F.; Botta, M. Parallel solution-phase synthesis of 4-dialkylamino-2-methylsulfonyl-6-vinyl-pyrimidines. *J. Comb. Chem.* **2005**, *7*, 117–122.
- (21) Das, K.; Bauman, J. D.; Clark, A. D., Jr.; Frenkel, Y. V.; Lewi, P. J.; Shatkin, A. J.; Hughes, S. H.; Arnold, E. High-resolution structures of HIV-1 reverse transcriptase/TMC278 complexes: Strategic flexibility explains potency against resistance mutations. *Proc. Natl. Acad. Sci. U.S.A.* **2008**, *105*, 1466–1471.
- (22) Esnouf, R. M.; Ren, J.; Hopkins, A. L.; Ross, C. K.; Jones, E. Y.; Stammers, D. K.; Stuart, D. I. Unique features in the structure of the complex between HIV-1 reverse transcriptase and the bis(heteroaryl)-piperazine (BHAP) U-90152 explain resistance mutations for this nonnucleoside inhibitor. *Proc. Natl. Acad. Sci. U.S.A.* **1997**, *94*, 3984–3989.
- (23) Himmel, D. M.; Das, K.; Clark, A. D., Jr.; Hughes, S. H.; Benjahad, A.; Oumouch, S.; Guillemont, J.; Coupa, S.; Poncelet, A.; Csoka, I.; Meyer, C.; Andries, K.; Nguyen, C. H.; Grierson, D. S.; Arnold, E. Crystal structures for HIV-1 reverse transcriptase in complexes with three pyridinone derivatives: a new class of non-nucleoside inhibitors effective against a broad range of drug-resistant strains. *J. Med. Chem.* **2005**, *48*, 7582–7591.
- (24) (a) Das, K.; Bauman, J. D.; Rim, A. S.; Dharia, C.; Clark, A. D.; Camarasa, M. J.; Balzarini, J.; Arnold, E. Crystal structure of tert-butylidimethylsilyl-spiroaminoxythioloedioxide-thymine (TSAO-T) in complex with HIV-1 reverse transcriptase (RT) redefines the elastic limits of the non-nucleoside inhibitor-binding pocket. *J. Med. Chem.* **2011**, *54*, 2727–2737. (b) Bailey, C. M.; Sullivan, T. J.; Iyidogan, P.; Tirado-Rives, J.; Chung, R.; Ruiz-Caro, J.; Mohamed, E.; Jorgensen, W.; Hunter, R.; Anderson, K. S. Bifunctional inhibition of human immunodeficiency virus type 1 reverse transcriptase: Mechanism and proof-of-concept as a novel therapeutic design strategy. *J. Med. Chem.* **2013**, *56*, 3959–3968.
- (25) Du, Q.-S.; Wang, Q.-Y.; Du, L.-Q.; Chen, D.; Huang, R.-B. Theoretical study on the polar hydrogen- π (H π) interactions between protein side chains. *Chem. Cent. J.* **2013**, *7* (92), 1–8.
- (26) Phillips, J. C.; Braun, R.; Wang, W.; Gumbart, J.; Tajkhorshid, E.; Villa, E.; Chipot, C.; Skeel, R. D.; Kale, L.; Schulten, K. J. Scalable molecular dynamics with NAMD. *Comput. Chem.* **2005**, *26*, 1781–1802.
- (27) Humphrey, W.; Dalke, A.; Schulten, K. J. VMD: Visual molecular dynamics. *Mol. Graphics* **1996**, *14*, 33–38.
- (28) Cornell, W. D.; Cieplak, P.; Bayly, C. I.; Gould, I. R.; Merz, K. M., Jr.; Ferguson, D. M.; Spellmeyer, D. C.; Fox, T.; Caldwell, J. W.; Kollman, P. A. A second generation force field for the simulation of proteins, nucleic acids, and organic molecules. *J. Am. Chem. Soc.* **1995**, *117*, 5179–5197.
- (29) Jorgensen, W. L.; Chandrasekhar, J.; Madura, J. D.; Impey, R. W.; Klein, M. L. Comparison of simple potential functions for simulating liquid water. *J. Chem. Phys.* **1983**, *79*, 926–935.
- (30) Schmidt, M. W.; Baldridge, K. K.; Boatz, J. A.; Elbert, S. T.; Gordon, M. S.; Jensen, J. H.; Koseki, S.; Matsunaga, N.; Nguyen, K. A.; Su, S.; Windus, T. L.; Dupuis, M.; Montgomery, J. A. General atomic and molecular electronic structure system. *J. Comput. Chem.* **1993**, *14*, 1347–1363.
- (31) Bayly, C. I.; Cieplak, P.; Cornell, W. D.; Kollman, P. A. A well behaved electrostatic potential based method using charge restraints for deriving atomic charges: the RESP model. *J. Phys. Chem.* **1993**, *97*, 10269–10280.
- (32) Tuckerman, M.; Berne, B.; Martyna, G. Reversible multiple time scale molecular dynamics. *J. Chem. Phys.* **1992**, *97*, 1990–2001.
- (33) Essman, U.; Perera, L.; Berkowitz, M. L.; Darden, T.; Lee, H.; Pedersen, L. A smooth particle mesh Ewald method. *J. Chem. Phys.* **1995**, *103* (19), 8577–8593.
- (34) Grest, G. S.; Kremer, K. Molecular dynamics simulation for polymers in the presence of a heat bath. *Phys. Rev. A* **1986**, *33*, 3628–3631.
- (35) Feller, S. E.; Zhang, Y.; Pastor, R. W.; Brooks, B. R. Constant pressure molecular dynamics simulation: the Langevin piston method. *J. Chem. Phys.* **1995**, *103*, 4613–4621.